Molecular Structure and Antioxidant Properties of Delphinidin

Laura Estévez and Ricardo A. Mosquera*

Departamento de Química Física, Facultade de Química, Universidade de Vigo, Lagoas-Marcosende s/n 36310-Vigo, Galicia, Spain

Received: May 15, 2008; Revised Manuscript Received: July 21, 2008

Density functional theory calculations were performed to evaluate the antioxidant activity of delphinidin, taking into account its acid/base equilibrium. The conformational behavior of both the isolated and the aqueous solvation species (simulated with the polarizable continuum model) were analyzed at the B3LYP/6-31++G(d,p) level, considering the cationic, neutral, and anionic forms, the latter two forms consisting of diverse tautomers. The analysis of their electron density distributions, using the quantum theory of atoms in molecules, reveals several facts that are not in line with their usual Lewis structures. The prototropic preferences observed in the gas phase and in solution are similar. Thus, in both phases, most stable tautomer of neutral delphinidin is obtained by deprotonating the hydroxyl at C4′, and the most stable tautomer of the anion is obtained by deprotonating the hydroxyls at C4′ and C5. All the planar conformers obtained display an intramolecular hydrogen bond (IHB) between O3 and H6′. Furthermore, the most stable tautomers of the neutral and anionic forms display two IHBs between O4′ and H3′ and H5′. To obtain ionization potentials (IPs) and homolytic O−H bond dissociation enthalpies (BDEs), the corresponding radical species were optimized at the UB3LYP level. Heterolytic O−H bond dissociation enthalpies (proton dissociation enthalpies, PDEs) were also computed. The expected important antioxidant activity can be justified from these results. IP, O−H BDE, and O−H PDE values suggest that one-step H atom transfer rather than sequential proton loss−electron transfer or electron transfer−proton transfer would be the most favored mechanisms for explaining the antioxidant activity of delphinidin in nonpolar solvents as well as in aqueous solution.

Introduction

A number of epidemiological studies summarized in diverse papers[1,2] have built the consensus that diets rich in fruits and vegetables have beneficial effects on human health. The subsequent decrease in the risk of certain pathologies, including cardiovascular diseases and cancer, is attributed in part to phenolic compounds contained in such food. Those molecules have demonstrated multiple biological properties including antioxidant activities.[3] Also, attention has increased mostly in finding naturally occurring antioxidants for use in foods or medicinal materials to replace synthetic antioxidants that, in some cases, have been reported to be carcinogenic.[4]

Anthocyanins represent one of the most widely distributed classes of flavonoids and are usually considered among the most important families of natural antioxidants. They belong to the group of polyphenolic antioxidants since they contain at least one hydroxyl group attached to a benzene ring and have been reported to possess antioxidant properties in vitro.[5−7]

According to the literature,[8−11] at least three mechanisms are involved in the radical-scavenging properties of phenolic antioxidants (ArOH). One involves a direct H atom transfer (HAT)[12] to the radical ($R^{\bullet}$), eq 1, another involves electron transfer−proton transfer (ET−PT), eq 2, and the third one, eq 3, has been termed sequential proton loss−electron transfer (SPLET) and takes place once the anion (ArO^-) has been formed. All of them (mechanisms 1−3) may occur in parallel, but with different rates.

$$R^{\bullet} + ArOH \rightarrow ArO^{\bullet} + RH \quad (1)$$

$$ArOH + R^{\bullet} \rightarrow ArOH^{\bullet+} + R^- \rightarrow ArO^{\bullet} + RH \quad (2)$$

$$ArOH \rightarrow ArO^- + H^+; \quad ArO^- + R^{\bullet} \rightarrow ArO^{\bullet} + R^-; \quad R^- + H^+ \rightarrow RH \quad (3)$$

The reaction implicated in mechanism 1 is governed by the bond dissociation enthalpy (BDE) of ArOH and RH. To a first approximation, if the BDE of the former is less than that of the latter, the reaction is permitted. The first step in mechanism 2 is an electron-transfer reaction, whose corresponding controlling parameters are the ionization potential (IP) of ArOH and R^-. A prerequisite for this reaction would be that the IP of the former is lower than that of R^-. Finally, the O−H heterolytic bond dissociation enthalpy (proton dissociation enthalpy, PDE) is involved in mechanism 3, where the IP of ArO^- is another controlling parameter.

The literature data on the antioxidant activity of anthocyanins are difficult to interpret because different methods are used to determine their antioxidant potency. Thus, different sequences of antioxidant activity have been reported in the literature.[5,13−15] This may in part be related to the many different forms in which anthocyanins may exist at different pH values.[16,17] This possible pH dependence of the radical-scavenging ability of anthocyanins possesses high interest because the pH range of different human body fluids is known to vary widely from pH 1 in the stomach to pH 5.3 in the small intestine, pH 6.8 in mouth saliva, pH 7.4 in blood and tissue fluid, pH 8 in the large intestine, pH 7−8.7 in the pancreas, and pH 8.3−9.3 in the duodenum.[18]

Even though anthocyanins generally occur as 3-*O*-glycosides, their bioactivity is attributed to the aglycon but not to the sugar or other binding species.[19] Therefore, the computational study

* To whom correspondence should be addressed. E-mail: mosquera@uvigo.es.

10.1021/jp8043237 CCC: $40.75
Published on Web 09/27/2008

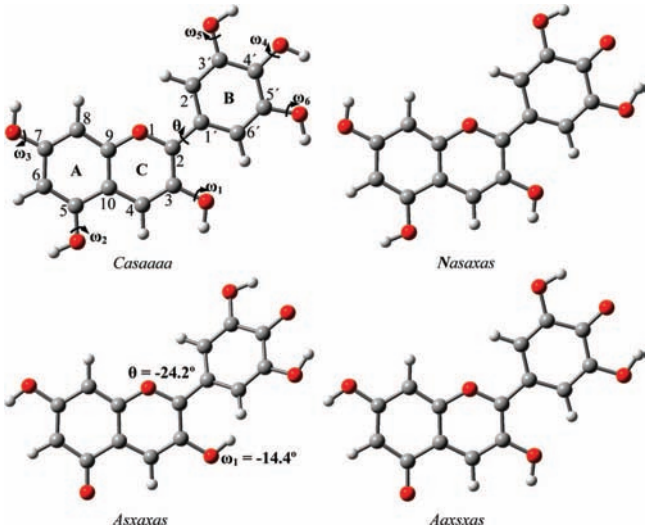

Figure 1. Most stable rotamer of the cationic, *Casaaaa*, neutral, *Nasaxas*, and anionic (nonplanar in the gas phase, *Asxsxas*, and planar, *Aaxsxas*, in solution) forms of delphinidin, showing the labeling scheme for the three rings (A, B, C), atom numbering, and main dihedral angles ($\omega_1-\omega_6$ and θ).

of these compounds can be concentrated on the aglycons, which are known as anthocyanidins.

Delphinidin (Figure 1) is the most common anthocyanidin molecule in blue flowers and forms with pelargonidin and cyanidin the three anthocyanidins known as the principal and basic skeletons of flower color pigments, so they are the most widespread in nature. To the best of our knowledge, despite the detailed theoretical studies available dealing with conformational aspects, O−H BDE, IP, and O−H PDE, in the gas phase,[20−30] there is a lack of corresponding studies in solution. In this context, we highlight that the IP and PDE values calculated for the isolated pelargonidin[31] (denoted subsequently as the "gas phase") and its "solution phase" counterpart, calculated with the polarizable continuum model (PCM),[32] differ significantly. Thus, for the cation of pelargonidin we obtained an IP value of 246.5 kcal mol^{-1} in the gas phase and 136.1 kcal mol^{-1} in solution. The same trend was found for the neutral (154.2 and 117.8 kcal mol^{-1}, respectively), whereas the reverse trend was observed for the anionic form (74.3 and 107.1 kcal mol^{-1}). In contrast, the 3-O−H PDE computed for the solvated cation exceeds that of the gas phase (282.3 (291.4) and 247.8 kcal mol^{-1}, respectively), whereas the reverse trend is observed for the neutral (287.3 (296.6) and 320.9 kcal mol^{-1}) and anionic forms (291.6 (300.9) and 389.2 kcal mol^{-1}). Also, significant changes are found between gas-phase and PCM electron density distributions of the neutral and ionic forms (vide infra). Nevertheless, similar O−H BDEs were obtained in both phases. Therefore, pointing to a better understanding of delphinidin antioxidative activity, and to contribute to the analysis of how the relative weight of the diverse mechanisms involved depends upon the pH and solvent, we have examined first the conformational and structural characteristics as well as the analysis of their electron distribution (with the quantum theory of atoms in molecules, QTAIM,[33] analysis) in the gas phase and in an aqueous solution of the cationic, neutral, and anionic forms of delphinidin acid/base equilibrium. Then, we have computed their IPs and all the corresponding BDEs and PDEs for every O−H group in both phases, which are compared to those of other phenolic antioxidants.[34]

Computational Details

The conformations of delphinidin are named by acronyms made by an italic capital letter indicating the concrete acid/base form of delphinidin considered (*C* = cation, *N* = neutral, *A* = anion) and six lower case letters indicating approximated values of the main dihedral angles defining the orientation of the hydroxyl groups. They are ω_1 (C2−C3−O−H), ω_2 (C5−C6−O−H), ω_3 (C6−C7−O−H), ω_4 (C3′−C4′−O−H), ω_5 (C2′−C3′−O−H), and ω_6 (C4′−C5′−O−H); *s* denotes nearly synperiplanar and *a* nearly antiperiplanar. Another important dihedral angle is O1−C2−C1′−C2′, hereafter denoted θ, which defines the coplanarity of the AC and B systems (Figure 1). Bearing in mind the different numbers of OH groups presented by the *C*, *N*, and *A* forms and the presence of multiple tautomers in *N* and *A*, the position of the symbol *x* indicates which hydroxyl has been deprotonated.

In our conformational analysis we have considered all the conformations obtained by combining *a* and *s* arrangements of ω_1, ω_2, and ω_3, whereas for the hydroxyls bonded to the B ring ($\omega_4-\omega_6$) we have only considered those combinations that maximize the number of intramolecular hydrogen bonds (IHBs).

The initial conformations of the different forms of delphinidin (cation, neutral, and anion) were fully optimized with the B3LYP[35] hybrid density functional by using the 6-31++G(d,p) basis set as implemented in the Gaussian 03 package.[36] The optimized structures were confirmed as true minima by vibrational analysis at the same level. Solvation free energies were computed using PCM[32] on the geometries optimized with this method.

Electron densities obtained at the same level, in the gas phase as well as in solution, were analyzed within the context of the QTAIM[33] using the AIMPAC program.[37] We focus on atomic populations, $N(\Omega)$, of the electron density.[33] Integration errors $[N - \sum N(\Omega)]$ were always smaller (in absolute value) than 4×10^{-3} au. All atoms were integrated with absolute atomic values of the *L* function, $|L(\Omega)|$,...,[33] lower than 0.002 au.

IPs and O−H BDEs were obtained by carrying out unrestricted UB3LYP/6-31++G(d,p) complete optimizations for the radical species obtained as a result of the ionization or O−H bond cleavage experienced by the most stable conformer of each of the delphinidin forms. IPs and BDEs, in the gas phase, were obtained including ZPVE and other thermal corrections to the enthalpy (TCE) of the final and initial states. As previously proposed,[38] we have employed gas-phase corrections to calculate these parameters in the aqueous phase because the calculation of vibrational frequencies with PCM is not very accurate and thermal corrections are expected to be rather similar in the gas and solvated phases. Alternatively, we also present the results obtained for the aqueous solution employing exclusively PCM total Gibbs energies in solution, G_{sol}.[34a]

Results and Discussion

Conformational and Electronic Distribution Analyses. In polyphenolic compounds, the behavior of the different OH groups is largely influenced by the neighboring groups and by the geometry. Thus, conformation can be regarded as the first parameter of importance to analyze the antioxidant capacity of delphinidin in its acid/base forms.

A detailed conformational analysis was performed for the three forms of delphinidin (cation, neutral, and anion) both in the gas phase and in a water solution modeled with PCM. The most important results are presented below in separate sections for the cationic, neutral, and anionic forms.

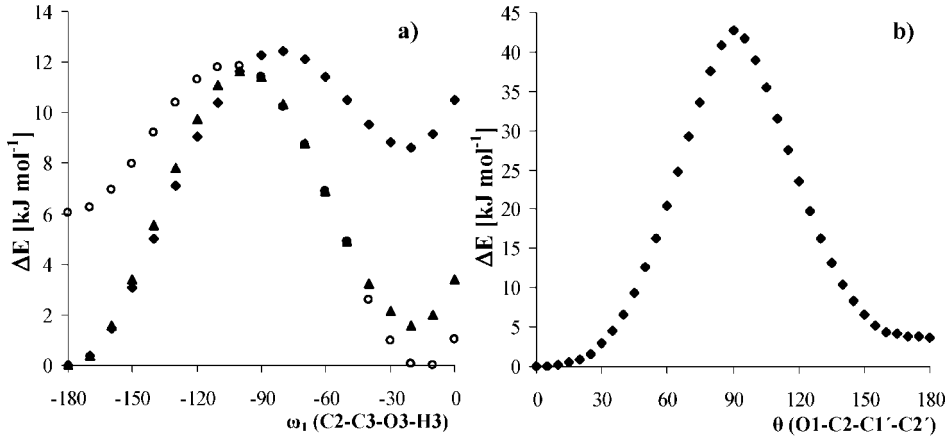

Figure 2. (a) Energy profiles (kJ mol^{-1}) for the internal rotation around ω_1 (C2−C3−O3−H3) for the most stable rotamer of the cationic, *Casaaaa* (solid squares), neutral, *Nasaxas* (solid triangles), and anionic, *Aaxsxas* (open circles), forms of delphinidin on going to *Cssaaaa*, *Nssaxas*, and *Asxsxas*, respectively, in the gas phase. (b) Energy profile (kJ mol^{-1}) for the internal rotation around θ (O1−C2−C1′−C2′) on going from *Casaaaa* to *Casaasss* in the gas phase.

Previous studies[28] and expected high repulsions between H6′ and H3 when ω_1 is in the *s* arrangement lead to the assumption of the *a* disposition for ω_1 in all the initial conformations. Nevertheless, we have checked the validity of this assumption for the cationic form and for every tautomer of the neutral and anionic forms (see below).

Cationic Form. According to the general rules indicated in the Computational Details, we have optimized eight different initial conformations (Table 1). The eight rotamers are completely planar, with the AC bicycle and the B ring sharing the same plane. The rotamer *Casaaaa* (Figure 1) has been found as the most stable conformer of this form in the gas phase. For this conformer, the internal rotation around ω_1 is hindered by a 3.0 kcal mol^{-1} barrier (Figure 2a) and leads to a shallow minimum (*Cssaaaa*), whose relative energy is 2.0 kcal mol^{-1}, confirming previous results[28] and qualitative expectations. This shallow minimum is not planar, showing a distorted B ring in response to the orientation of the 3-OH group ($\omega_1 = 20.0°$, $\theta = 29.7°$). We remark that both the relative energy of the *Cs*----- rotamer and this energy barrier increase drastically when the 3-OH group is replaced by a methoxyl unit to model the corresponding anthocyanin. Also, important structural variations and a significant rise of the molecular energy are expected for the 3-*O*-glucoside forms.[28]

The internal rotation around the C2−C1′ bond (Figure 2b) gives rise to another planar rotamer (*Casasss*) whose relative energy is 1 kcal mol^{-1} (Table 1). The corresponding energy barrier is 10.2 kcal mol^{-1}, suggesting hindered rotation at room temperature.

As observed in our previous paper on pelargonidin[31] the relative energies of the *Caa*---- rotamers are higher (between 4.8 and 6.0 kcal mol^{-1} in delphinidin) than those of the corresponding *Cas*---- structures, and therefore, the *Caa*---- rotamers were confirmed as transition states. Also, the bond lengths and bond angles are scarcely affected by conformational changes. In fact, the largest variation of the bond lengths, observed for C9−C10, is only 0.010 Å.

The electron density analysis carried out with QTAIM indicates—by finding a bond path—that all the *Ca*----- rotamers display an O3···H6′−C6′ IHB. This IHB modifies the C6′−H6′ vibrational frequency, ν(C6′−H6′), which is 3267.8 cm^{-1} in *Casaaaa* and displays rather slight variations for the other conformers of the delphinidin cation. In contrast, when this IHB is not present, like in the equivalent conformer of the 3-deoxydelphinidin or in the *Cssaaaa* rotamer (which we use as references for analysis of red/blue shifts because this IHB is not possible), ν(C6′−H6′) is significantly smaller (3215.1 and 3201.1 cm^{-1}, respectively). Also, the C6′−H6′ bond length is shorter in the *Ca*----- (1.080 Å) series than in the *Cs*----- series (1.085 Å) and in 3-deoxydelphinidin (1.084 Å), indicating the formation of a *blue-shifted* IHB.

Nevertheless, the expected IHBs between adjacent hydroxyls of the B ring are not represented by bond paths in the QTAIM analysis. The same fact was reported for glucopyranose,[39] other saturated 1,2-diols,[40,41] and cathecol.[41] In spite of the lack of IHB bond paths, there are noticeable differences in the frequencies of the hydroxyl groups. Looking at the frequencies, we observe that the 3′-OH ($\nu_{O-H} = 3757.8$ cm^{-1}) and 4′-OH ($\nu_{O-H} = 3780.8$ cm^{-1}) stretchings are lower than those of OH groups which are not expected to form IHBs (3835.1 cm^{-1} < ν_{O-H} < 3806.1 cm^{-1}). Also, the bond lengths of the former O−H groups are longer, another characteristic of a *red-shifted* IHB (for more details see the Supporting Information). It can also be noticed that, in spite of the lack of an IHB bond path, IHB energies were assigned by Mandado et al.[42] in simple diols to justify the larger stability of some conformers.

The eight stationary points found in the gas phase were also optimized by simulating the aqueous solvation with the PCM method. The lowest energy in PCM is shared by two rotamers, *Casaaaa* and *Casasss*. The relative energy of the other *Cas*---- rotamers is less than 0.1 kcal mol^{-1}. In contrast, the four *Caa*---- rotamers display imaginary frequencies and a relative energy above 3.3 kcal mol^{-1}. We notice that the relative energies are shrunk by PCM with regard to the gas phase, as the usual consequence of the interactions of every OH group with the solvent. The largest polarization stabilization takes place when ω_2 is anti (*Caa*---- series). The polarization energy also stabilizes the *C---sss* series more than the *C---aaa* series (Table 1).

The geometries are nearly unaffected by PCM calculations (the largest variations are displayed by the O−H bond lengths—between 0.012 and 0.023 Å—whereas those of the backbone are below 0.008 Å (C2−C1′) and 8.8° (C6−C7−O7). This is also true for all the properties associated with IHBs, where we observe a slight decrease of the electron density (less than 4×10^{-4} au) at the bond critical point (BCP), accompanied by a slight increase of the IHB bond length (less than 0.015 Å).

Comparing solution and gas-phase electron densities, analyzed within the framework of QTAIM, we notice that polarization of the molecule increases in solution. This trend is especially

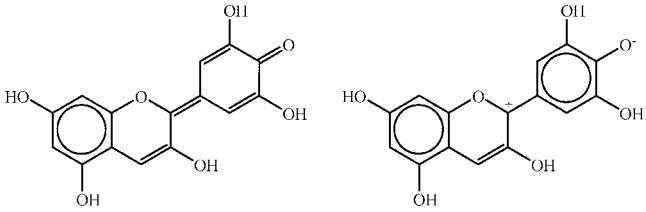

Figure 3. Some resonance structures for the **N4′** neutral form of delphinidin. Other enolate resonance structures (not shown) place the positive charge on O1, C4, C5, C7, C9, C2′, C4′, and C6′.

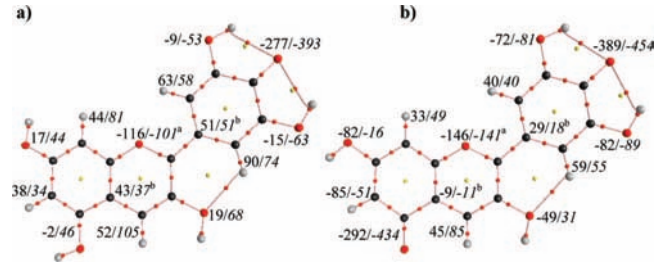

Figure 4. Molecular graphs (obtained with AIM-2000[50]) for the most stable rotamers of tautomers **N4′** (neutral) (a) and **A54′** (anion) (b) of delphinidin. The values are referred to formal global charges (multiplied by 10^3) for each C−H and C−O−H unit in the gas phase (values in solution in italics). Notes: a, C2−O1−C9 unit; b, global charge of the carbon atom.

intense for hydroxyl groups, whose N(O) values increase between 0.03 and 0.05 au, whereas the N(H) values are depleted by a similar amount. Overall, the positive charge of the cation, in the gas phase, as previously obtained for flavylium and pelargonidin cations,[29] is not placed on O1, but is distributed all over the molecule (global charges of the AC and B systems are, respectively, 0.559 and 0.445 au) with an important contribution (more than 30%) from hydrogens bonded to carbon atoms. This shows that resonance forms are inadequate for qualitative descriptions of the electron distribution of these systems. PCM simulation enlarges the positive charge of the AC bicycle (0.652), transferring electron density to the B ring (almost 0.1 au). Looking at $N(\Omega)$, we notice all N(H) values become depleted in solution. This depletion is more intense in the hydrogens bonded to carbons of the AC system (0.083 au in total), which is nearly the electron density transferred to the B ring upon solvation, than in those of the B ring (0.025 au in total), whereas N(C3′) displays the largest increase.

Neutral Form. The delphinidin cation studied above is the main form in strong acidic media. This cation is transformed into the neutral form upon deprotonation when the pH is raised. As delphinidin has six OH groups, we can distinguish six different neutral tautomers which henceforth will be named by the atom attached to the carbonyl oxygen. Every one of them appears as a set of rotamers.

The **N4′** tautomer is found as the most stable one and presents two rotamers that are nearly isoenergetic (*Nasaxas* and *Nassxas*, referred to hereafter as the most stable neutral structures). The energies of the remaining tautomers are higher than 6.0 kcal mol^{-1} after ZPVE corrections, and those tautomers should not be present in the gas-phase equilibrium mixture. The most stable rotamers for those tautomers are *Nssxsss* for **N7**, *Naxsaaa* for **N5**, *Nxsaaaa* for **N3**, and *Nssasxs* and *Nssaaax* for **N3′** and **N5′**, respectively, whose relative energies are higher than 15.0 kcal mol^{-1}. The most stable conformers of the **N4′**, **N5**, and **N3** tautomers are planar (Supporting Information), the *Nxs*---- rotamers of **N3** being true conformers, contrary to what is found for the remaining tautomers and cation.

As a general trend the tautomerism of the neutral forms gives rise to variations in the bond lengths of the polycyclic system, which are practically unaffected by internal rotation of the hydroxyls. In agreement with our previous work on pelargonidin,[31] the largest variations are displayed up to three bonds from the deprotonation site and basically agree with the predictions (within these three bonds) of the resonance model (Supporting Information).

The term quinonoidal assigned to the neutral form of anthocyanins and anthocyanidins comes from the fact that it is usually represented by a quinonoidal Lewis structure containing a C═O double bond (shown in Figure 3 for **N4′**). The comparison of bond lengths between the most stable neutral and cationic rotamers, *Nasaxas* and *Nasaaaa*, respectively, is the main support for this quinonoidal structure. Thus, we observe significant changes in the bond lengths of the AC−B system (Supporting Information). The most important ones are localized in the B ring and in the C2−C1′ bond (as could be deduced from their commonly accepted Lewis structures), which gets closer to a double bond (becoming 1.400 Å upon a 0.042 Å reduction from the cation). Nevertheless, several resonance forms (see Figure 3 and the Supporting Information) displaying positive and negative sites—enolate-like structures—can be drawn for neutral anthocyanins. Moreover, taking into account previously observed shortcomings when resonance forms are employed for qualitative descriptions of electron distributions, we think that the electron distribution of neutral anthocyanidin species should be analyzed with some detail before accepting that they bear a quinonoidal structure.

We observe that C4′−O4′ displays negative charge (−0.277 au), whereas the corresponding COH group in the cation is slightly positive (0.087 au). To propose that enolate-like forms play a significant role in neutral delphinidin, we should also find a significant positive charge distributed on certain atoms, C2, C4, C5, C7, C9, C2′, C4′, and C6′, but not on others, C3, C6, C8, C10, C1′, C3′, and C5′. Some QTAIM electron populations are not in line with this rule, e.g., N(C1′) < N(C2′), N(C10) < N(C4), etc. The resonance description differs even more from the QTAIM results when the atomic populations are summed into C−H, C−O−H, and C−O−C groups. Then we notice that the C−O−H groups are nearly neutral (their charges differing from zero by less than 0.02 au) and there are two negatively charged regions (the C4′−O4′ and the C2−O1−C9 units), counterbalanced by the three remaining areas in the molecules (Figure 4). Overall, in spite of their geometry, neutral forms of delphinidin display a certain enolate character, bearing a negative charge around the deprotonated oxygen, which is counterbalanced in a fashion different from that expected from the enolate-like resonance forms.

All the *Na*----- and *Nx*----- neutral rotamers display (as commented above for the cation) O3···H6′−C6′ hydrogen bonding (detected as a QTAIM bond path). It is noticeable that this IHB is still blue-shifted in the *Na*----- rotamers but not in the rotamers of the **N3** tautomers (*Nx*-----). Thus, ν(C6′−H6′) is 3287.4 cm^{-1} in the former and 3191.8 cm^{-1} in the latter with C6′−H6′ bond lengths of 1.078 and 1.085 Å, respectively. In the corresponding 3-deoxydelphinidin, ν(C6′−H6′) is 3221.4 cm^{-1} and the C6′−H6′ bond length is 1.083 Å. Furthermore, interatomic distances and ρ_{BCP} values indicate this IHB is stronger when O3 is deprotonated, 2.019 Å and 26.4 × 10^{-3} au, respectively. For the other tautomers these values go from 2.085 to 2.113 Å and from 19.4 × 10^{-3} to 21.0 × 10^{-3} au. Also, the **N3′**, **N4′**, and **N5′** tautomers display other IHBs involving the carbonyl and the adjacent hydroxyl groups, all of

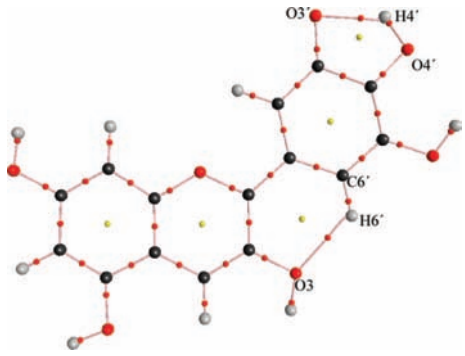

Figure 5. Molecular graph (obtained with AIM-2000[50]) for the most stable rotamer, *Nasasxs*, of the **N3′** tautomer of delphinidin computed from its completely optimized B3LYP/6-31++G(d,p) electron density. The molecular graph contains the bond paths associated with the O3···H6′−C6′ IHB and with the O3′···H4′−O4′ IHB. Notice that neither the BCP nor the bond path is detected for the expected H4′−O4′···H5′−O5′ IHB.

TABLE 1: B3LYP/6-31++G(d,p) Relative Energies (kcal mol^{-1}) for Isolated and Solution Rotamers of the Delphinidin Cation

rotamer	ΔE^a	ΔE^b	$\Delta E^{PCM\ a}$	$E^{PCM} - E^{gas\ b}$	ΔG_{sol}	E_{pol}
Casaaaa	0.00	0.00	0.00	−74.4	−71.3	−81.8
Cassaaa	0.58	0.50	0.12	−74.9	−72.6	−83.0
Casasss	0.88	0.82	0.01	−75.3	−72.9	−83.3
Casssss	1.04	0.95	0.10	−75.3	−73.2	−83.6
Caasaaa[c]	5.55	5.28	3.56	−76.4	−72.6	−83.4
Caassss[c]	5.84	5.20	3.53	−76.7	−75.2	−85.7
Caaaaaa[c]	5.95	5.70	3.53	−76.8	−73.3	−84.1
Caaasss[c]	6.66	5.93	3.53	−77.5	−76.7	−87.2

[a] the energies are relative to the most stable conformer with no ZPVE corrections. This reference is E(*Casaaaa*) = −1104.61397 au in the gas phase and E(*Casaaaa*) = −1104.73253 au in the PCM-modeled aqueous solvated phase. [b] The energies are relative to the most stable conformer with ZPVE corrections. This reference is E(+ZPVE)(*Casaaaa*) = −1104.37269 au. [c] This rotamer presents one imaginary frequency.

them represented by a bond path. Nevertheless, we have not found any bond path for the expected IHBs between two adjacent hydroxyl groups (Figure 5). It is noticeable that the *Ns*----- rotamers, which are nonplanar, do not display any bond path associable with the O3···H6′-C6′ IHB.

PCM optimizations agree with gas-phase optimizations in that the *Nasaxas* rotamer of the **N4′** tautomer is the most stable neutral structure. Again, the PCM results indicate a general reduction of relative energies among the tautomers and also among the rotamers. Thus, the relative energy of the least stable conformers (those with the highest dipole moment) is the most reduced by solvation (Table 2) because of their electrostatic interactions with the solvent molecules.

Nevertheless, the difference from the energy of the next tautomer is still higher than 4.4 kcal mol^{-1}. There is a significant modification of the relative energies in **N3** because of the largest polarization energy shown by the *Nx---ss* series of rotamers. A similar trend is observed when the polarization energies of *Naxsss* and *Nax-aaa* are compared for the **N5** tautomer. Contrary to what is found in the gas phase, PCM optimizations favor planar anti arrangements around ω_1. Thus, the nonplanar gas geometry of the *Nssxsss* rotamer gives rise after PCM optimization to *Nasxsss* (Table 2).

Comparing the solution and gas-phase geometries, we observe some equalization of the C−C bond lengths, lengthening the shortest ones and shrinking the longest ones in PCM. This equalization is especially intense for the bond lengths of the B ring. Looking at the corresponding QTAIM atomic properties of PCM-optimized electron densities, we notice significant changes in some atomic electron populations. Changes can be summarized as electron density transference from the AC system to the hydrophilic part of the B ring. In contrast with the gas phase, the C−O−H units become significantly charged (negative in B and positive in AC) with PCM electron densities. We also observe that N(O4′) is substantially larger in PCM than in the gas phase (9.241 and 9.172 au, respectively), whereas the reverse trend is observed for N(C2) (5.474 and 5.515 au), which could be interpreted as the PCM electron distribution enhancing the weight of enolate-like forms. In contrast, N(O1) is nearly constant (9.126 au in PCM and 9.123 au in the gas phase).

It should be noticed that the detection of BCPs associated with the IHBs involving hydroxyls adjacent to the carbonyl group depends on how the cavity around the molecule is built up. Thus, when it is constructed by superimposing individual spheres for every atom (including hydrogens), those BCPs are found, and they are not detected with a cavity obtained with the simple united atomic topological model (UAO). On the contrary, the H6′···O3−H3 BCP is always detected.

Anionic Form. Neutral forms are transformed into anions upon deprotonation of another hydroxyl in basic media. There are 15 possible tautomers, which we name by indicating after a capital **A** the atoms attached to the two dehydroxylated oxygens. The rotamers are named as in the previous forms. Once again, we explored the conformational preference of ω_1 (syn or anti) (see below) for the 10 tautomers keeping the 3-OH group. Most of the rotamers where ω_2 is antiperiplanar are transition states. Nevertheless, this orientation is a minimum (whose energy is even lower than that of the corresponding syn rotamer) in the C3-deprotonated tautomers (as observed in the neutral forms) excluding the **A37** tautomers.

As in pelargonidin,[31] **A54′** is the most stable tautomer, displaying in the gas phase a significant preference for the *Asxsxas* rotamer (Table 3). It is followed by **A74′** in the stability sequence, which displays a clear preference for the *Assxxas* rotamer. The next tautomer is **A34′** (its rotamer *Axaaxas* has a relative energy of 3.0 kcal mol^{-1}). The relative energies of all the rotamers of the remaining tautomers are over 8 kcal mol^{-1}, and therefore, those tautomers will be considered negligible in the equilibrium mixture. It is noticeable that when the two protons are taken from the B ring, the syn arrangement of O4′−H is the only one which yields all the real frequencies.

The profiles of the energy for the internal rotation of the ω_1 dihedral angle were obtained for the most stable rotamer of each tautomer which keeps the 3-OH group. As can be observed (Supporting Information), only the **A57** tautomer presents a planar structure in the minimum. For the most stable tautomer ω_1 is −10.0°, and as a consequence the B ring becomes distorted and θ reaches −25.1° (Figure 2). On the other hand, the **A3** tautomers are completely planar (θ = 0.0°).

As was found for the neutral forms, tautomerism gives rise to important variations in the bond lengths of the polycyclic system (Supporting Information). Comparing the most stable planar rotamer of the neutral, *Nasaxas*, and anion, *Aaxsxas*, forms, we observe changes in the bond lengths of the whole AC−B system. Although the main differences are observed for the A ring (C5−C10 and C5−C6 lengthen), important changes are also observed in the C (C4−C10 shrinks) and B (C4′−O4′ lengthens by 0.022 Å) systems. Compared to the most stable rotamer of the cation, we notice different shrinkages for the

TABLE 2: B3LYP/6-31++G(d,p) Relative Energies (kcal mol^{-1}) in the Gas Phase and in PCM-Modeled Aqueous Solvated Neutral Delphinidin Rotamers

tautomer	rotamer	$\Delta E^{\text{gas}\ a}$	$\Delta E^{\text{gas}\ b}$	$\Delta E^{\text{PCM}\ a}$	tautomer	rotamer	$\Delta E^{\text{gas}\ a}$	$\Delta E^{\text{gas}\ b}$	$\Delta E^{\text{PCM}\ a}$
N4′	*Nasaxas*	0.00	0.00	0.00	**N5**	*Naxasss*	8.83	8.00	5.09
N4′	*Nassxas*	1.01	0.90	0.10	**N3**	*Nxsasss*	9.71	9.04	5.07
N4′	*Naaaxas*[c]	3.18	2.65	3.02	**N3**	*Nxssssss*	10.39	9.62	5.26
N4′	*Naasxas*[c]	3.28	2.77	3.03	**N7**	*Naaxsss*[c]	12.95	12.00	7.79
N3	*Nxsaaaa*	6.59	6.18	4.89	**N7**	*Naaxaaa*[c]	13.42	12.43	7.81
N5	*Naxsaaa*	6.64	6.03	4.59	**N5′**	*Nssaaax*	15.23	15.00	12.08
N5	*Naxssss*	6.73	6.14	4.57	**N3′**	*Nssasxs*	16.01	15.79	11.76
N3	*Nxasaaa*	7.33	6.64	7.74	**N5′**	*Nsssaax*	16.19	15.16	12.14
N7	*Nssxsss*	7.48	7.28	6.12	**N3′**	*Nssssxs*	17.23	16.42	11.82
N3	*Nxssaaa*	7.66	7.10	5.10	**N3′**	*Nasasxs*	17.12	16.31	9.42
N7	*Nasxsss*	8.03	7.83	4.39	**N3′**	*Nasssxs*	18.46	17.49	9.59
N5	*Naxaaaa*	8.36	7.57	5.07	**N5′**	*Nasaaax*	19.17	18.14	10.19
N7	*Nasxaaa*	8.42	7.71	4.40	**N5′**	*Nassaax*	20.21	19.05	10.33
N7	*Nssxaaa*	8.55	7.84	6.15					

[a] The energies are relative to the most stable conformer with no ZPVE corrections. This reference is $E(Nasaxas) = -1104.22034$ au in the gas phase and $E(Nasaxas) = -1104.27943$ au in the PCM-modeled aqueous solvated phase. [b] The energies are relative to the most stable conformer with ZPVE corrections. This reference is $E(+\text{ZPVE})(Nasaxas) = -1103.99177$ au in the gas phase. [c] This structure displays one imaginary frequency associated with ω_2.

TABLE 3: B3LYP/6-31++G(d,p) Relative Energies (kcal mol^{-1}) in the Gas Phase and in Solution for Rotamers of the Anionic Form of Delphinidin

tautomer	rotamer	ΔE^{a}	ΔE^{b}	$\Delta E^{\text{PCM}\ a}$	$E^{\text{PCM}} - E^{\text{gas}\ b}$	ΔG_{sol}	E_{pol}
A54′	*Asxsxas*	0.00	0.00	2.29	−60.8	−61.3	−72.6
A74′	*Assxxas*	1.39	1.42	2.08	−62.3	−63.3	−74.7
A54′	*Aaxsxas*	1.47	0.97	0.00	−64.5	−63.1	−74.3
A54′	*Aaxaxas*	2.33	1.69	0.43	−64.9	−64.3	−75.5
A34′	*Axaaxas*	3.73	3.04	2.62	−64.2	−65.5	−76.8
A74′	*Aasxxas*	4.22	3.61	0.40	−66.9	−68.5	−79.6
A34′	*Axsaxas*	6.28	5.68	0.41	−68.9	−72.5	−83.7
A34′	*Axssxas*	7.69	6.88	0.60	−70.1	−75.2	−86.4
A74′	*Aaaxxas*[c]	7.83	6.49	3.62	−67.3	−71.2	−82.4

[a] The energies are relative to the most stable conformer with no ZPVE corrections. This reference is $E(Asxsxas) = -1103.71056$ au in the gas phase and $E(Aaxsxas) = -1103.81103$ au in aqueous solution PCM modeling. [b] The energies are relative to the most stable conformer with ZPVE corrections. This reference is $E(+\text{ZPVE})(Asxsxas) = -1103.49474$ au. [c] This rotamer presents one imaginary frequency.

deprotonated OH groups of the most stable anion (−0.093 and −0.069 Å for C5−O5 and C4′-O4′, respectively).

QTAIM analysis indicates the negative charge is mainly spread among three regions of the anion (Figure 4b): the two C−O units where hydrogens have been removed (−0.292 au in C5−O5 and −0.389 au for C4′−O4′ in the most stable tautomer) and the C2−O1−C9 area (−0.146 au). Whereas the bond lengths and group charges could be interpreted in support of the predominance of the resonance form that leaves a negative charge on O4′, N(O5) exceeds N(O4′). Also, some results, such as the negative charge of the C2−O1−C9 unit, which is more negative than in the neutral form, are not in line with any of the possible resonance forms for describing this anion.

All the anionic rotamers *Aa*----- and *Ax*----- (as commented on for previous forms) display O3···H6′−C6′ hydrogen bonding (detected as a bond path), and as in the neutral form, this IHB is blue-shifted for *Aa*----- but not for *Ax*-----. The interatomic distances and ρ_{BCP} values indicate this IHB is stronger when O3 is deprotonated (**N3** tautomers), as in the neutral form. Thus, ρ_{BCP} is between 2.31×10^{-2} and 2.34×10^{-2} au in these tautomers and goes from 1.80×10^{-2} to 1.90×10^{-2} au when O3 is protonated. $R_{\text{O3}\cdots\text{H6}'}$ is shorter than 2.090 Å for the O3-deprotonated forms and longer than 2.137 Å for the O3-protonated forms. The **A3′**, **A4′**, and **A5′** tautomers display other IHBs detected as bond paths between the carbonyl group in the 3′, 4′, or 5′ position and the hydrogen of the adjacent hydroxyl group. As in previous forms (Figure 5), no bond path associated with BCP between adjacent hydroxyl groups has been detected.

The energetic trends among anions are retained on going from the gas phase to the aqueous solution, but relative energies among the tautomers are lower. In solution, planar structures are stabilized with regard to the corresponding nonplanar structure. For example, the most stable anion in solution, *Aaxsxas*, is stabilized by more than 2.2 kcal mol^{-1} with regard to *Asxsxas*, the most stable in the gas phase, because of the polarization (−74.3 vs −72.6 kcal mol^{-1}) and solvation (−63.1 vs −61.3 kcal mol^{-1}) energies.

Comparing the solution and gas-phase geometries, we observe a general increase of the bond lengths, with the exception of the C−C bonds of the C−C═O units. Also, as commented on for the neutral forms, the detection of bond paths associated with IHB is affected by the model employed to build the molecular cavity.

The main difference found between group populations in PCM and the gas phase is the enlargement of the electron density of the deprotonated hydroxyls (Figure 4b), whose negative charges represent more than 88% of the molecular charge. This electron density is taken from the rest of the molecule with no noteworthy exception.

Homolytic and Heterolytic O−H Breaking. ***Cationic Form.*** Homolytic breaking of O−H bonds in the delphinidin cation can give rise to six different radicals, named using the numbering of the broken OH group as **RC3**, **RC5**, **RC7**, **RC3′**, **RC4′**, and **RC5′**. The order of stability for the radical species obtained from the most stable rotamer of the cation in the gas phase (*Casaaaa*) is **RC4′** > **RC3** > **RC3′** > **RC5′** > **RC5** > **RC7**. Homolytic breaking of the 4′-OH hydroxyl is favored by the double cathecol moiety. **RC3**, which is stabilized by the C6′−H6′···O3 IHB, lies at 4.5 kcal mol^{-1} with respect to the global minimum **RC4′** (Table 4). It can be observed that the stability sequence for the **RC** species differs slightly from that displayed by the species formed by heterolytic breaking of one O−H bond, proton abstraction, which is the stability sequence for the tautomers of the neutral delphinidin: **N4′** > **N3** > **N5** > **N7** > **N3′** > **N5′** (Table 2). We notice that both O−H breaking energies are computed as energy differences between rotamers

TABLE 4: Relative Enthalpies,[a] ΔH, for the Radicals Obtained from the Most Stable Cation, Neutral, and Anion of Delphinidin in the Gas Phase and in Aqueous Solvation at the B3LYP/6-31++G(d,p) Level[b]

Casaaaa	ΔH^{gas}	ΔH^{PCM}	*Nasaxas*	ΔH^{gas}	ΔH^{PCM}	*Aaxsxas*	ΔH^{gas}	ΔH^{PCM}
RC4′	0.00	0.00 (0.00)						
RC3	4.51	5.71 (5.98)	**RN3**	0.00	0.00 (0.00)	**RA3**	0.00	0.00 (0.00)
RC3′	7.19	6.38 (7.32)	**RN3′**	13.54	4.45 (4.75)	**RA3′**	14.66	6.14 (6.48)
RC5′	7.31	6.31 (6.60)	**RN5′**	13.29	3.87 (4.13)	**RA5′**	13.18	5.88 (6.18)
RC5	11.94	9.73 (10.63)	**RN5**	5.17	4.28 (4.64)			
RC7	14.07	10.21 (10.86)	**RN7**	4.56	2.89 (3.08)	**RA7**	14.66	7.12 (7.75)

[a] Obtained from the total electronic energies corrected with TCE terms as explained in the text for gas-phase and PCM calculations. [b] PCM relative energies obtained from the total Gibbs energies, ΔG, are given in parentheses. All values are in Kcal mol^{-1}.

which may involve conformational changes. Thus, for **N4′** and **RC4′** the final states are, respectively, *Nasaxas* and *RCasaxas*, whereas the initial state is *Casaaaa*. This means that an internal rotation around ω_7 (hindered by only 2.6 kcal mol^{-1}) is coupled to the O−H breaking. Moreover, restricted homolytic or heterolytic 4′-OH breaking with a frozen geometry (transformation of *Casaaaa* into *RCasaxaa* or *Nasaxaa*, respectively) destabilizes **RC4′** and **N4′** by 6.4 and 7.5 kcal mol^{-1}, respectively, which would modify the stability sequence.

The order of the relative stabilities of the radicals obtained for the aqueous phase with PCM is basically the same as that in the gas phase. In fact, the unique change observed affects **RC3′** and **RC5′**, which are practically isoenergetic in both phases (Table 4). In contrast, the order obtained with PCM for the neutral species formed after proton abstraction is altered, **N4′** > **N7** > **N5** > **N3** > **N3′** > **N5′** (Table 2), which can be related to the different influence of PCM upon charged and uncharged species involved in a heterolytic breaking.

Neutral Form. The most stable tautomer of the neutral form, **N4′** (rotamer *Nasaxas*), gives rise to five different radicals upon homolytic H abstraction. The most stable one, in the gas phase, is that obtained by breaking the 3-OH group (**RN3**). Radicals resulting from breaking 7-OH, 5-OH, 5′-OH, and 3′-OH are found, respectively, 4.6, 5.2, 13.3, and 13.5 kcal mol^{-1} above the global minimum (Table 4). The rather low stability of the **RN3′** and **RN5′** species can be attributed to the proximity between the two deprotonated oxygen atoms, which bear large negative charges.

In contrast, the relative energy of the anions formed upon H^+ removal from *Nasaxas* indicates that the 3-, 5-, and 7-OH positions are nearly isoenergetic (anionic tautomers **A34′**, **A54′**, and **A74′**). **A3′4′** and **A4′5′** display higher relative energies, above 23.9 kcal mol^{-1} (see Table 3).

In the PCM optimizations the most stable radical from *Nasaxas* is **RN3**, and **RN7** is the next one (2.9 kcal mol^{-1} above), as in the gas phase. There is a reduction in the relative energies of the **RN3′** and **RN5′** radicals, whose relative preference is also altered with regard to the gas phase. Thus, we found that **RN5′** is the third most stable radical with a relative energy of 3.9 kcal mol^{-1}, being nearly isoenergetic to the **RN5** and **RN3′** radicals.

As commented on in the previous section, the sequence of the relative energies of the anionic species formed upon H^+ removal from *Nasaxas* is the same as in the gas phase.

Anionic Form. Homolytic breaking of the 3-OH bond in the most stable tautomer of anionic delphinidin, **A54′** (rotamer *Asxsxas*), gives rise to its most stable radical. It is remarkable that all these **RA3** radicals are completely planar. The other three possible radicals are more than 13.1 kcal mol^{-1} higher in energy.

The most stable dianion, obtained after H^+ removal from *Asxsxas*, is formed by heterolytic breaking of the 7-OH hydroxyl. It is followed by the dianion obtained by breaking the 3-OH hydroxyl (2.2 kcal mol^{-1} higher). Dianions formed from 3′-OH and 5′-OH are 19.9 and 17.8 kcal mol^{-1} higher, respectively.

TABLE 5: IP and O−H BDE Values for Delphinidin (D) in Its Different Forms, Cation (C), Neutral (N), and Anion (A), in the Gas Phase and in Aqueous Solvation Simulated with PCM (Italic) at the B3LYP/6-31++G(d,p) Level[a]

	D(C)	D(N)	D(A)
IP	240.7/*133.3*	150.0/*112.5*	73.2/*103.6*
O−H BDE (3)	80.0/*81.2* (89.6)	69.1/*72.1* (80.4)	61.3/*67.1* (75.1)
O−H BDE (5)	87.4/*85.2* (94.2)	74.3/*76.4* (85.1)	
O−H BDE (7)	89.6/*85.7* (94.5)	73.6/*75.0* (83.5)	76.1/*74.3* (82.9)
O−H BDE (4′)	75.5/*75.5* (83.6)		
O−H BDE (3′)	82.7/*81.9* (90.9)	82.6/*76.6* (85.2)	77.7/*73.3* (81.6)
O−H BDE (5′)	82.8/*81.8* (90.2)	82.4/*76.0* (84.6)	77.4/*73.0* (81.3)

[a] PCM values of BDEs obtained from the total free energies (ΔG) are given in parentheses. All values are in Kcal mol^{-1}.

The sequence of the stability of the radical species obtained from *Aaxsxas* in PCM calculations is the same as in the gas phase, but with smaller relative energies (Table 3).

According to PCM, the most stable dianion, obtained from *Aaxsxas*, is formed at the 3-OH position, followed by that formed at 7-OH (0.6 kcal mol^{-1} higher). The 3′-OH and 5′-OH dianions are 8.5 and 9.6 kcal mol^{-1} higher, respectively. Once more, we observe that PCM reduces the differences in the relative energies and in this case also gives a different order of the stability sequence of the dianions.

Ionization Potential and O−H Bond Dissociation Enthalpy. As mentioned previously, phenolics and flavonoids can play their protective role by donating a H atom or acting as electron donors. It is clear that the BDE for the O−H bond and the IP are of particular importance for selecting the most favored mechanism for the radical-scavenging activity. We have computed the BDE and IP not only in the gas phase but also in aqueous solution since water is the main component of physiological liquids.

Adiabatic IPs were calculated in the gas phase for the most stable structure of the cation, neutral, and anion forms of delphinidin as the differences between the electronic energy of the corresponding ionized form, E^+, and that of the parent species, E_p, corrected with ZPVE. As could be expected, the sequence for the IPs is cation > neutral > anion (Table 5).

The IP of the cation is significantly larger (240.8 kcal mol^{-1}) than those of widely used food synthetic additives such as butylated hydroxyanisole, propyl gallate, and nordihydroguaiaretic acid (respectively, 152.7, 167.8, and 160.6 kcal mol^{-1})[8] and the natural polyphenolic flavonoid epigallocatechin-3-gallate (147.7 kcal mol^{-1}), one of the most active antioxidants obtained from green tea.[34b] Even the IP of neutral delphinidin (150.0 kcal mol^{-1}) is comparable to those indicated above.

IPs obtained from PCM calculations are significantly modified with regard to those obtained in the gas phase, because of the stabilization experienced by charged systems in polar solvents. Thus, values of 133.3, 112.5, and 103.7 kcal mol^{-1} are obtained for the cation, neutral, and anion forms, respectively.

BDEs were calculated for each OH group of the most stable cation (*Casaaaa*), neutral form (*Nasaxsa*), and anion (*Asxaxsa*) of delphinidin in the gas phase. For this calculation we have also included TCE corrections. BDE is calculated as the enthalpy difference at 298 K for reaction 1.

BDEs computed in the gas phase are similar to or smaller than (61.3−89.6 kcal mol^{-1}) those of hydroxybenzoic or cinnamic acid (83.7−105.6 kcal mol^{-1})[34c,d] and phenol (values varying from 82.7 to 87.6 kcal mol^{-1} depending upon the method employed).[43] As a general trend BDEs computed for each position follow the sequence cation > neutral > anion. The lower the pH, the easier the H atom abstraction. We notice that 4′-OH displays the lowest BDE for the cation, while 3-OH represents the easiest H abstraction for the neutral and anionic forms.

Two procedures (see the Computational Details) have been applied to obtain BDEs in aqueous solution. BDEs computed as the difference between the total Gibbs energies in solution values, $\Delta_{BDE}G_{sol}$, are systematically 8−9 kcal mol^{-1} larger than those computed with PCM total electronic energies and gas-phase thermal enthalpy corrections, $\Delta_{BDE}H^{PCM*}$. As shown in Table 5, the $\Delta_{BDE}H^{PCM*}$ values are very similar to gas-phase BDEs, whereas the $\Delta_{BDE}G_{sol}$ values exceed them by more than 10%. Anyway, the most favorable sites for H abstraction remain unchanged from the gas phase to aqueous solution (4′-OH for the cation and 3-OH for the other forms).

The effect of the conformation on the antioxidant activity was tested by computing O−H BDEs in the gas phase for another rotamer of the cation (*Cassaaa*). The results indicate that the orientation of the hydroxyl bond to C7 lowers the BDE of the hydroxyl at C5 by 2.3 kcal mol^{-1}. The BDE of the hydroxyl at C7 is modified by 0.5 kcal mol^{-1}, whereas the BDEs of the remaining hydroxyls are practically unaffected (less than 0.2 kcal mol^{-1}).

Antioxidant Mechanisms. According to Wright et al.,[34e] the mechanism dominating the antioxidant activity of a certain phenolic compound can be inferred from the relative values of its IP and BDE with regard to phenol[44] (ΔIP and ΔBDE, respectively). Thus, HAT dominates when ΔIP ≥ −36 kcal mol^{-1} and ΔBDE is around −10 kcal mol^{-1}, whereas electron transfer is predominant when ΔIP ≤ −45 kcal mol^{-1}. Therefore, our results for the gas phase would indicate that the preferred antioxidant mechanism of delphinidin is HAT for cations, while electron-transfer processes would become the most important mechanisms for anions. In contrast, HAT and electron-transfer processes would take place simultaneously and competitively for the neutral forms. Nevertheless, the gas-phase results would only simulate the behavior in nonpolar solvents, where the uncharged forms would be preferred. Thus, we should look at PCM-computed IPs and BDEs, where we observe that all ΔIP values are above −33.3 kcal mol^{-1}, which would point to HAT as always being the most favored antioxidant mechanism for delphinidin.

Another distinction should be made: it is common that delphinidin (like other anthocyanidins) occurs as its 3-*O*-glycoside. This fact produces a significant effect on pelargonidin because the lowest ΔBDE of its neutral form corresponds to 3-OH (ΔBDE = −11.3 kcal mol^{-1}), while for its 3-*O*-glycoside derivative (pelargonin) the lowest ΔBDE corresponds to 4′-OH (−4.8 kcal mol^{-1}), making the HAT mechanism more difficult. Nevertheless, this is not the case for delphinidin because the second lowest BDEs (7-OH for the neutral form and 5′-OH for the anion) display ΔBDE values (−9.5 and −11.5 kcal mol^{-1}, respectively) which verify the Wright et al.[34e] condition.

TABLE 6: O−H PDE Values for Delphinidin (D) in Its Different Forms, Cation (C), Neutral (N), and Anion (A), in the Gas Phase and in Aqueous Solvation Simulated with PCM (Italic) at the B3LYP/6-31++G(d,p) Level[a]

	D(C)	D(N)	D(A)
O−H PDE (3)	246.5/*282.1* (291.1)	250.0/*287.0* (296.2)	388.4/*293.2* (300.7)
O−H PDE (5)	248.2/*282.3* (291.3)	250.0/*287.1* (296.2)	
O−H PDE (7)	248.4/*281.7* (290.6)	250.1/*287.2* (296.1)	386.2/*293.8* (301.7)
O−H PDE (3′)	256.7/*286.3* (295.5)	258.5/*295.5* (305.7)	406.1/*301.7* (297.8)
O−H PDE (4′)	240.3/*277.6* (286.2)		
O−H PDE (5′)	258.5/*286.9* (296.3)	259.8/*296.8* (307.1)	404.0/*302.8* (310.5)

[a] PDE values obtained from the total free energy (Δ*G*) are given in parentheses. All values are in Kcal mol^{-1}.

The SPLET mechanism (3) is quoted by several authors.[9−11] In this case, the control parameters are the IP of the species formed after deprotonation and the O−H PDE (see below) giving rise to this species. The analysis of our results, according to the Wright et al.[34e] condition for the electron transfer, and taking into account the relatively low O−H PDEs found for the three species (lower than that of several polyphenols),[45] shows that this mechanism may be possible for both the cation and neutral forms in the gas phase (ΔIP = −40.7 and −114.9 kcal mol^{-1}, respectively, for the deprotonated species formed). The results from aqueous solution calculations indicate that no species will act as radical scavengers through the SPLET mechanism (ΔIP = −24.4 and −33.3 kcal mol^{-1}, respectively, for the neutral and anion species formed after deprotonation).

Overall, following the Wright et al.[34e] conditions, the HAT mechanism seems to be the only one practicable or the preferred one. However, it should be kept in mind that the relative importance of HAT, ET−PT, or SPLET is not only determined by microenvironmental features (lipid phase, aqueous phase) but also governed by the characteristics of the scavenged radical.[11] Besides structural characteristics, we need to consider how the electron affinity and H atom affinity of the radical species, R$^{\bullet}$, reacting with our anthocyanidin affects the three mechanisms, and even how the electron densities of both compounds evolve along the reaction.[46]

Finally, another antioxidant mechanism is related to the ability of anthocyanidins to chelate transition-metal ions, which gives rise to stable complexes that prevent these metals from participating in free radical generation.[47] In fact, during the Fenton reaction (4),[48] hydroxyl radicals are produced from hydrogen peroxide in the presence of a metal in a low oxidation state.

$$H_2O_2 + M^{n+} \rightarrow HO^- + OH^{\bullet} + M^{(n+1)+} \quad (4)$$

In the "metal chelation" mechanism, the loss of a proton by the polyphenol is crucial for its antioxidant ability, because the cation's chelation often involves at least one deprotonated ligand.[49] Therefore, the acidity of these compounds is an important parameter to be taken into account, since the smaller the OH group acidity, the easier the deprotonation and the metal chelation. Therefore, we calculated the OH proton dissociation enthalpy O−H PDE (Table 6), defined as $H_d + H_{proton} - H_p$, in which H_d is the enthalpy of the molecule derived from proton dissociation, H_{proton} is the enthalpy of the proton (−0.00236 au),

TABLE 7: $\Delta_{PDE}G$ Values and Corresponding Relative Acidities (with Regard to Phenol)[44] Computed for the Deprotonations of the Main Forms of Delphinidin[a]

	Casaaaa		*Nasaxas*		*Asxsxas*	
	$\Delta_{PDE}G$	relative pK_a	$\Delta_{PDE}G$	relative pK_a	$\Delta_{PDE}G$	relative pK_a
3-OH	−14.3	−10.4	−9.2	−6.7	−4.7	−3.4
5-OH	−14.1	−10.3	−9.2	−6.7		
7-OH	−14.8	−10.8	−9.3	−6.8	−3.7	−2.7
3′-OH	−9.9	−7.2	0.3	0.2	−7.6	−5.5
4′-OH	−19.2	−14.0				
5′-OH	−9.1	−6.6	1.7	1.2	5.1	3.7

[a] All values are in Kcal mol^{-1}.

and H_p is the enthalpy of the parent molecule. For the calculations in the condensed phase, the acidities were computed in the same terms and also in terms of ΔG_{sol}. pK_a values in solution were obtained (Table 7) from the relative total free energies using an expression previously proposed in the literature.[45]

Conclusions

According to our B3LYP/6-31++G(d,p) study, the following conclusions on the molecular structure of delphinidin can be obtained.

(1) The most stable rotamers of the cation and neutral forms of delphinidin are completely planar in the gas phase, while the anion is significantly distorted from planarity. In contrast, the most stable rotamers of the three forms are planar according to PCM calculations.

(2) *Casaaaa* is found as the most stable rotamer of the cation in the gas phase. The internal rotations around the C3−O3 and C5−O5 bonds result in very significant destabilizations. When 3-OH is substituted by a bulkier group (it is usually substituted by a glycoside in delphinins), the rotation around this bond is even more restricted.

(3) **N4′**, displaying two HB bond paths between O4′ and the hydroxyls at C3′ and C5′, is the most stable tautomer of neutral delphinidin in the gas phase. This tautomer shows a preference (by ca. 1 kcal mol^{-1}) for the syn disposition of the C6−C7−O−H dihedral angle. The remaining tautomers are found at least 4 kcal mol^{-1} above the *Nasaxas* conformer.

(4) **A54′** is found as the most stable tautomer of the anion in the gas phase, although the relative energy of one rotamer of **A74′** (*Assxxas*) is only 1.42 kcal mol^{-1}. **A54′** displays a significant preference for the *Asxsxas* rotamer. The relative energies of the **A34′** rotamers are above 3 kcal mol^{-1}, whereas those of the remaining tautomers are higher than 8 kcal mol^{-1}.

(5) Conformational relative energies are generally reduced by PCM optimizations. The sequence of conformational energies is altered for the cation. *Casaaaa* remains as the most stable rotamer but is nearly isoenergetic with *Casasss*. In the neutral form, the sequence of stability does not change within the four most stable rotamers. However, there is an interchange in the relative position of some other neutral tautomers. Furthermore, the nonplanar *Nssxsss* rotamer of **N7** tautomer in the gas phase becomes more stable in its planar conformation *Nasxsss* than some **N3** or **N5** rotamers. Planar structures of the anions are stabilized in aqueous solution with regard to the corresponding nonplanar structure. Thus, *Aaxsxas* becomes the most stable rotamer, because of its high polarization and solvation energies.

(6) All the planar rotamers of each form and tautomer of delphinidin display an intramolecular hydrogen bond between O3 and H6′ represented by a bond path. This IHB is accompanied by a clear blue shift of the frequency associated with C6′−H6′ stretching when O3 belongs to a hydroxyl group, but not when the hydroxyl has been deprotonated. Possible IHBs connecting adjacent hydroxyls are not represented by a bond path. In contrast, this kind of bond path is observed when one of the hydroxyls has been deprotonated.

(7) According to the QTAIM analysis performed here, the following conclusions can be made: (i) The positive charge of the cation is placed neither on O1 nor in the C2−O1−C9 unit, but is distributed between the AC system and the B ring, with an important contribution from hydrogens bonded to carbon atoms. (ii) The neutral forms show two negatively charged areas, the deprotonated hydroxyl and teh C2−O1−C9 unit, with the rest of the molecule bearing a positive charge. Overall, the electronic distribution of the neutral form differs from that of a quinonoidal structure and could be described as an enolate whose negative charge is counterbalanced by diverse regions which are positively charged. (iii) The negative charge of the anionic forms is basically spread among three areas, the two C−O units where protons have been removed and the C2−O1−C9 unit. Electron distributions obtained with PCM calculations differ from those in the gas phase by an increased polarization, which gives rise to a certain electron transference from the AC system to the B ring (cation and neutral forms) and a significant increase of the negative charge at the deprotonated hydroxyls in the anion.

(8) 4′ is the most favored site for homolytic O−H breaking in the cation, whereas 3 is preferred for the most stable tautomers of the neutral and anionic forms. These preferences are the same in the gas and aqueous solution phases.

(9) Adiabatic IPs depend significantly on the phase because of the stabilization of charged species by polar solvents. Thus, the IPs of cation and neutral forms become significantly lower using PCM calculations (240.8 and 133.3 kcal mol^{-1} for the cation, 150.0 and 112.5 kcal mol^{-1} for the neutral form), while the reverse trend is observed for the anion (73.2 in the gas phase and 103.7 with PCM).

(10) PCM-computed values for IPs, BDEs, and PDEs, compatible with a high antioxidant activity, indicate that one-step HAT, rather than SPLET or ET−PT, is the most favored mechanism for explaining the radical-scavenger activity of delphinidin in aqueous solutions.

Acknowledgment. L.E. thanks the Universidade de Vigo for a predoctoral fellowship. We thank the Centro de Supercomputación de Galicia (CESGA) for free access to its computational facilities and the Spanish MEC for funding this research through Project CTQ2006-15500.

Supporting Information Available: Energy profiles for the internal rotation around C3−O3 for the most stable rotamer of different tautomers of neutral and anion forms of delphinidin, optimized O−H stretching vibrational frequencies for the most stable rotamer of the cation form, geometry details for the cation, neutral, and anion forms of delphinidin, and relative energies for all rotamers studied for the anion form of delphinidin. This material is available free of charge via the Internet at http://pubs.acs.org.

References and Notes

(1) Hertog, M. G. L.; Feskens, E. J. M.; Hollman, P. C. H.; Katan, M. B.; Kromhout, D. *Lancet* **1993**, *342*, 1007.
(2) Trichopoulou, A.; Vasilopoulou, E. *Br. J. Nutr.* **2000**, *84*, 205.
(3) Sarma, A. D.; Sharma, R. *Phytochemistry* **1999**, *52*, 1313.
(4) Zheng, W. S.; Wang, Y. *J. Agric. Food Chem.* **2001**, *46*, 5165.
(5) Wang, H.; Cao, G.; Prior, R. L. *J. Agric. Food Chem.* **1997**, *45*, 304.

(6) Pool-Zobel, B. L.; Bub, A.; Schroder, N.; Rechkemmer, G. *Eur. J. Nutr.* **1999**, *38*, 227.

(7) Tsuda, T.; Shiga, K.; Kawakishi, S.; Osawa, T. *Biochem. Pharmacol.* **1996**, *52*, 1033.

(8) Zhang, H.-Y.; Sun, Y.-M.; Wang, X.-L. *Chem.—Eur. J.* **2003**, *9*, 502 and references therein.

(9) Nakanishi, I.; Kawashima, T.; Ohkubo, K.; Kanazawa, H.; Inami, K.; Mochizuki, M.; Fukuzumi, S.; Ikota, N. *Org. Biomol. Chem.* **2005**, *3*, 626.

(10) Musialik, M.; Litwinienko, G. *Org. Lett.* **2005**, *7*, 4951.

(11) Zhang, H.-Y.; Ji, H.-F. *New J. Chem.* **2006**, *30*, 503.

(12) This pathway is also called electron-coupled proton transfer or proton-coupled electron transfer: Mayer, J. M.; Rhile, I. J. *Biochim. Biophys. Acta* **2004**, *1655*, 51.

(13) Rice-Evans, C. A.; Miller, N. J.; Paganga, G. *Free Radical Biol. Med.* **1996**, *20*, 933.

(14) Rice-Evans, C. A.; Miller, N. J.; Bolwell, P. G.; Bramley, P. M.; Pridham, J. B. *Free Radical Res.* **1995**, *22*, 375.

(15) Lapidot, T.; Harel, S.; Akiri, B.; Granit, R.; Kanner, J. *J. Agric. Food Chem.* **1999**, *47*, 67.

(16) Heredia, F. J.; Franchia-Aricha, E. M.; Rivas-Gonzalo, J. C.; Vicario, I. M.; Santos-Buelga, C. *Food Chem.* **1998**, *63*, 491.

(17) Brouillard, R. In *Anthocyanins as Food Colors*; Markasis P., Ed.; Academic Press: New York, 1982; p 1.

(18) Grzymislawski, M. In *Human Nutrition. Principals of Nutritional Science* (in Polish); Gawęcki, J., Hryniewiecki, L., Eds.; PWN: Warsaw, Poland, 2000; p 56.

(19) Sakakibara, H.; Ashida, H.; Kanazawa, K. *Free Radical Res.* **2002**, *36*, 307.

(20) Kurtin, W. E.; Song, P.-S. *Tetrahedron* **1968**, *24*, 2255.

(21) Rastelli, G.; Costantino, L.; Albasini, A. *J. Mol. Struct.* **1993**, *279*, 157.

(22) Pereira, G. K.; Donate, P. M.; Galembeck, S. E. *J. Mol. Struct.: THEOCHEM* **1997**, *392*, 169.

(23) Figueiredo, P.; Elhabiri, M.; Saito, N.; Brouillard, R. *Phytochemistry* **1995**, *41*, 301.

(24) Pereira, G. K.; Donate, P. M.; Galembeck, S. E. *J. Mol. Struct.: THEOCHEM* **1996**, *363*, 87.

(25) Mateus, M.; Carvalho, E.; Carvalho, A. R. F.; Melo, A.; González-Paramás, A. M.; Santos-Buelga, C.; Silva, A. M. S.; de Freitas, V. *J. Agric. Food Chem.* **2003**, *51*, 277.

(26) Meyer, M. *Int. J. Quantum Chem.* **2000**, *76*, 724.

(27) Woodford, J. N. *Chem. Phys. Lett.* **2005**, *410*, 182.

(28) Sakata, K.; Saito, N.; Honda, T. *Tetrahedron* **2006**, *62*, 3721.

(29) Estévez, L.; Mosquera, R. A. *Chem. Phys. Lett.* **2008**, *451*, 121.

(30) Borkowski, T.; Szymusiak, H.; Gliszczynska-Swiglo, A.; Rietjens, I. M. C. M.; Tyrakowska, B. *J. Agric. Food Chem.* **2005**, *53*, 5526.

(31) Estévez, L.; Mosquera, R. A. *J. Phys. Chem. A* **2007**, *111*, 11100.

(32) Tomasi, J.; Mennuci, B.; Cammi, R. *Chem. Rev.* **2005**, *105*, 2999.

(33) (a) Bader, R. F. W. *Chem. Rev.* **1991**, *91*, 893. (b) Bader, R. F. W. *Atoms in Molecules: A Quantum Theory*; Oxford University Press: New York, 1990.

(34) (a) Leopoldini, M.; Marino, T.; Russo, N.; Toscano, M. *J. Phys. Chem. A* **2004**, *108*, 4916. (b) Lien, E. J.; Ren, S.; Bui, H. -H.; Wang, R. *Free Radical Biol. Med.* **1999**, *26*, 285. (c) Mandado, M.; Graña, A. M.; Mosquera, R. A. *Chem. Phys. Lett.* **2004**, *400*, 169. (d) Gonzalez-Moa, M. J.; Mandado, M.; Mosquera, R. A. *Chem. Phys. Lett.* **2006**, *424*, 17. (e) Wright, J. S.; Johnson, E. R.; DiLabio, G. A. *J. Am. Chem. Soc.* **2001**, *123*, 1173.

(35) (a) Becke, A. D. *J. Chem. Phys.* **1993**, *98*, 5648. (b) Lee, C.; Yang, G.; Parr, R. G. *Phys. Rev.* **1988**, *37*, 785.

(36) Frisch, M. J.; Trucks, G. W.; Schlegel, H. B.; Scuseria, G. E.; Robb, M. A.; Cheeseman, J. R.; Montgomery, J. A., Jr.; Vreven, T.; Kudin, K. N.; Burant, J. C.; Millam, J. M.; Iyengar, S. S.; Tomasi, J.; Barone, V.; Mennucci, B.; Cossi, M.; Scalmani, G.; Rega, N.; Petersson, G. A.; Nakatsuji, H.; Hada, M.; Ehara, M.; Toyota, K.; Fukuda, R.; Hasegawa, J.; Ishida, M.; Nakajima, T.; Honda, Y.; Kitao, O.; Nakai, H.; Klene, M.; Li, X.; Knox, J. E.; Hratchian, H. P.; Cross, J. B.; Bakken, V.; Adamo, C.; Jaramillo, J.; Gomperts, R.; Stratmann, R. E.; Yazyev, O.; Austin, A. J.; Cammi, R.; Pomelli, C.; Ochterski, J. W.; Ayala, P. Y.; Morokuma, K.; Voth, G. A.; Salvador, P.; Dannenberg, J. J.; Zakrzewski, V. G.; Dapprich, S.; Daniels, A. D.; Strain, M. C.; Farkas, O.; Malick, D. K.; Rabuck, A. D.; Raghavachari, K.; Foresman, J. B.; Ortiz, J. V.; Cui, Q.; Baboul, A. G.; Clifford, S.; Cioslowski, J.; Stefanov, B. B.; Liu, G.; Liashenko, A.; Piskorz, P.; Komaromi, I.; Martin, R. L.; Fox, D. J.; Keith, T.; Al-Laham, M. A.; Peng, C. Y.; Nanayakkara, A.; Challacombe, M.; Gill, P. M. W.; Johnson, B.; Chen, W.; Wong, M. W.; Gonzalez, C.; Pople, J. A. *Gaussian 03*, revision C.02; Gaussian, Inc.: Wallingford, CT, 2004.

(37) Bader, R. F. W.; et al. *AIMPAC: A Suite of Programs for the Theory of Atoms in Molecules*; McMaster University: Hamilton, Ontario, Canada, 1994.

(38) Rezabal, E.; Mercero, J. M.; Lopez, X.; Ugalde, J. M. *J. Inorg. Biochem.* **2007**, *101*, 1192.

(39) Klein, R. A. *J. Am. Chem. Soc.* **2002**, *124*, 13931.

(40) Klein, R. A. *J. Comput. Chem.* **2002**, *23*, 585.

(41) Mandado, M.; Graña, A. M.; Mosquera, R. A. *Phys. Chem. Chem. Phys.* **2004**, *6*, 4391.

(42) Mandado, M.; Mosquera, R. A.; Van Alsenoy, C. *Tetrahedron* **2006**, *62*, 4243.

(43) (a) Wayner, D. D.; Lusztyk, E.; Ingold, K. U.; Mulder, P. *J. Org. Chem.* **1996**, *61*, 6430. (b) de Heer, M. I.; Korth, H. G.; Mulder, P. *J. Org. Chem.* **1999**, *64*, 6969.

(44) IP and OH BDE values computed by us at the B3LYP/6-31++g(d,p) level were, respectively, 190.7 and 82.4 kcal mol^{-1} for the gas phase and 137.5 and 84.0 kcal mol^{-1} in the aqueous phase with the PCM model (or 92.4 kcal mol^{-1}, obtained in terms of total free solvation energies).

(45) (a) Leopoldini, M.; Russo, N.; Toscano, M. *J. Agric. Food Chem.* **2006**, *54*, 3078. (b) Leopoldini, M.; Marino, T.; Russo, N.; Toscano, M. *Theor. Chem. Acc.* **2004**, *111*, 210.

(46) Singh, N.; O′Malley, P. J.; Popelier, P. L. A. *Phys. Chem. Chem. Phys.* **2005**, *7*, 614.

(47) Jocanovic, S. V.; Steenken, S.; Simic, M. G.; Hara, Y. In *Flavonoids in Health and Disease*; Rice-Evans, C., Packer, L., Eds.; Marcel Dekker: New York, 1998; p 137.

(48) (a) Brown, J. E.; Khodr, H.; Hider, R. C.; Rice-Evans, C. *Biochem. J.* **1998**, *330*, 1173. (b) van Acker, S. A. B. E.; van den Berg, D. J.; Tromp, M. N. J. L.; Griffaen, D. H.; van Bennekom, W. P.; van Vijgh, W. J. F.; Bast, A. *Free Radical Biol. Med.* **1996**, *20*, 331.

(49) Fernandez, M. T.; Mira, M. L.; Florêncio, M. H.; Jennings, K. R. *J. Inorg. Biochem.* **2002**, *92*, 105.

(50) Biegler-König, F. W.; Schönbohm, J.; Bayles, D. *J. Comput. Chem.* **2001**, *22*, 545.

JP8043237